THE ASTROPHYSICAL JOURNAL, 634:L49–L52, 2005 November 20

SIMULTANEOUS MULTIWAVELENGTH OBSERVATIONS OF SAGITTARIUS A*

T. AN,[1] W. M. GOSS,[2] JUN-HUI ZHAO,[3] X. Y. HONG,[1] S. ROY,[4] A. P. RAO,[4] AND Z.-Q. SHEN[1]

Received 2005 March 22; accepted 2005 October 10; published 2005 November 3

ABSTRACT

We observed Sgr A* using the Very Large Array (VLA) and the Giant Metrewave Radio Telescope (GMRT) at multiple centimeter and millimeter wavelengths on 2003 June 17. The measured flux densities of Sgr A*, together with those obtained from the Submillimeter Array (SMA) and the Keck II 10 m telescope on the same date, are used to construct a simultaneous spectrum of Sgr A* from 90 cm to 3.8 μm. The simultaneous spectrum shows a spectral break at about 3.6 cm, a possible signature of synchrotron self-absorption of the strong radio outburst that occurred near epoch 2003 July 17. At 90 cm, the flux density of Sgr A* is 0.22 ± 0.06 Jy, suggesting a sharp decrease in flux density at wavelengths longer than 47 cm. The spectrum at long cm wavelengths appears to be consistent with free-free absorption by a screen of ionized gas with a cutoff ~100 cm. This cutoff wavelength appears to be three times longer than that of ~30 cm suggested by Davies, Walsh, & Booth based on observations in 1974 and 1975. Our analysis suggests that the flux densities of Sgr A* at wavelengths longer than 30 cm could be attenuated and modulated by stellar winds from massive stars close to Sgr A*.

Subject headings: accretion, accretion disks — black hole physics — Galaxy: center — radio continuum: galaxies

1. INTRODUCTION

Soon after the discovery of the compact radio source Sagittarius A* at the Galactic center (Balick & Brown 1974) Davies et al. (1976, hereafter DWB) carried out observations of Sgr A* at 0.408, 0.96 and 1.66 GHz. Sgr A* was only detected at the two higher frequencies. The measurements showed a low-frequency turnover around 1 GHz in the spectrum of Sgr A*. The authors attributed the decrease in flux density below 1 GHz to free-free absorption from ionized gas of Sgr A West. Recent observations of Sgr A* at both 620 and 330 MHz indicate that the spectrum below 1 GHz may indeed have a pronounced turnover. At 620 MHz, Roy & Rao (2004) detected Sgr A* using the GMRT with a flux density of 0.5 ± 0.1 Jy and with an angular resolution of $11''.4 \times 7''.6$, while Nord et al. (2004) detected Sgr A* at 330 MHz using the VLA of the National Radio Astronomy Observatory (NRAO) with a flux density of 0.33 ± 0.12 Jy (resolution of ~9″).

Sgr A* is now believed to be associated with a supermassive black hole (SMBH) with a mass $\sim 4 \times 10^6\, M_\odot$ (Schödel et al. 2002; Ghez et al. 2003). A number of models have been proposed to explain the observed phenomena in the vicinity of Sgr A* at radio, near-IR, and X-ray wavelengths (Melia & Falcke 2001). Coker & Melia (1997) proposed that stellar winds, which originate from massive stars near Sgr A*, might play an important role in fuelling Sgr A* and therefore may have caused the variations in flux density at radio wavelengths. These models are sensitive to the observed spectrum of Sgr A*. Simultaneous multiwavelength observations could provide important constraints for current accretion or outflow theories. If stellar winds are indeed responsible for the flux density variations at millimeter/submillimeter wavelengths, a cutoff at long radio wavelengths could be sensitive to changes in stellar wind flux near Sgr A*.

To determine the low-frequency turnover in the spectrum of Sgr A*, we have performed multiwavelength observations using the VLA at 90, 26, 23, 20, 17, 6, 3.6, 2, 1.3, and 0.7 cm, and the GMRT at 47 cm on 2003 June 17 (UT). At the same epoch, both the SMA (Moran 1998; Ho et al. 2004) and the Keck II 10 m telescope observed Sgr A* at 0.89 mm and 3.8 μm, respectively. In this Letter, we present results from the quasi-simultaneous observations.

2. OBSERVATIONS AND DATA REDUCTION

The VLA and GMRT observations are summarized in Table 1, including observing band (λ), frequency (ν), bandwidth ($\Delta\nu$), on-source time (t), and flux density of the primary calibrator (S_c). The observations with the VLA were carried out in the A configuration at wavelengths from 90 cm to 7 mm. The observations at 90 and 20 cm with the VLA and at 47 cm with the GMRT were performed in spectral line modes in order to reject radio frequency interference and minimize bandwidth smearing. The raw data were reduced using the Astronomical Image Processing System (AIPS) of the NRAO following standard procedures. Absolute flux density calibration was performed using 3C 286 (at 0.7, 1.3, and 2 cm) or 3C 48 (at other wavelengths) following the flux density scales of Baars et al. (1977). The flux density calibration of 3C 48 or 3C 286 was carried out using the visibilities over appropriate u-v ranges suggested by VLA documentation at wavelengths between 90 and 2 cm; clean models of 3C 286 (obtained from C. Chandler) were used for flux density calibrations at 1.3 and 0.7 cm using all visibilities. A few nearby QSOs were interleaved during the observations of Sgr A* to determine the complex gains. An amplitude and phase calibration of 3C 48 or 3C 286 was performed using a 2 minute solution interval to obtain average flux density scales over the scan, which were then applied to the phase calibrators and Sgr A*. A few iterations of phase self-calibrations of calibrated u-v data were also performed to correct for residual phase errors. The GMRT calibration procedure for observation of the Galactic center is described in detail by Roy & Rao (2004). The primary flux density calibrator was 3C 48, whose flux density is 28.5 Jy at 640 MHz (Baars scale). Corrections were made for the increase of the system

[1] Shanghai Astronomical Observatory, Chinese Academy of Sciences, Shanghai 200030, China; antao@shao.ac.cn.
[2] National Radio Astronomy Observatory, P.O. Box O, Socorro, NM 87801.
[3] Harvard-Smithsonian Center for Astrophysics, 60 Garden Street, MS 78, Cambridge, MA 02138.
[4] National Center for Radio Astrophysics (TIFR), Pune University Campus, Post Bag 3, Ganeshkhind, Pune 411 007, India.

TABLE 1
OBSERVATIONAL DATA OF SGR A* ON 2003 JUNE 17

λ (cm)	ν (GHz)	Δν (MHz)	t (minutes)	S_c (Jy)
90	0.303/0.332	6	29	3C 48 (45.2/42.9)
47	0.640	16	85	3C 48 (28.5)
20[a]	1.16/1.30/1.50/1.74	34	56	3C 48 (18.6/17.0/15.2/13.5)
6	4.835/4.885	100	11	3C 48 (5.5/5.4)
3.6	8.435/8.485	100	11	3C 48 (3.2/3.1)
2	14.915/14.965	100	11	3C 286 (3.5/3.5)
1.3	22.435/22.485	100	29	3C 286 (2.52)
0.7	43.315/43.365	100	32	3C 286 (1.45)

Observations at 20 cm were carried out at four frequencies.

temperature in the direction of the Galactic center compared to the high Galactic latitude field of 3C 48. The point sources 1751−253 and 1741−25 were used as secondary phase and bandpass calibrators, respectively.

3. DATA ANALYSIS AND RESULTS

The flux densities of Sgr A* were determined in the image domain. Either a point-source or an elliptical Gaussian model was used to fit the data. The flux density measurement at 90 cm is discussed in § 3.1. At 20 cm, Sgr A* is slightly resolved; thus a two-dimensional elliptical Gaussian function was used to fit the long-baseline (>20 kλ) visibilities. At wavelengths between 6 and 0.7 cm, free-free emission from the H II regions in Sgr A West is resolved out on baselines longer than 80 kλ. The flux density of a point source can be directly determined in the *u-v* domain by averaging the amplitude of the visibilities on baselines >80 kλ. The difference in flux densities between the two procedures is consistent with the uncertainty (σ_M) in the measurements. The calibration uncertainty (σ_C) is dominated by the uncertainty in the calibration of the flux density scale. The final 1 σ errors are the quadrature addition of the two terms, i.e., $(\sigma_M^2 + \sigma_C^2)^{1/2}$. The measurements of flux densities at 2, 1.3, and 0.7 cm are consistent with the values derived from the VLA monitoring program (Herrnstein et al. 2004). The GMRT image at 47 cm was made with a *u-v* range 10–50 kλ to minimize confusion from the Sgr A complex. A Gaussian model was fitted to the flux density distribution of Sgr A* and a constant term with a slope was fitted to the background using `jmfit` in AIPS. The flux density of Sgr A* is 0.45 ± 0.10 Jy at 47 cm.

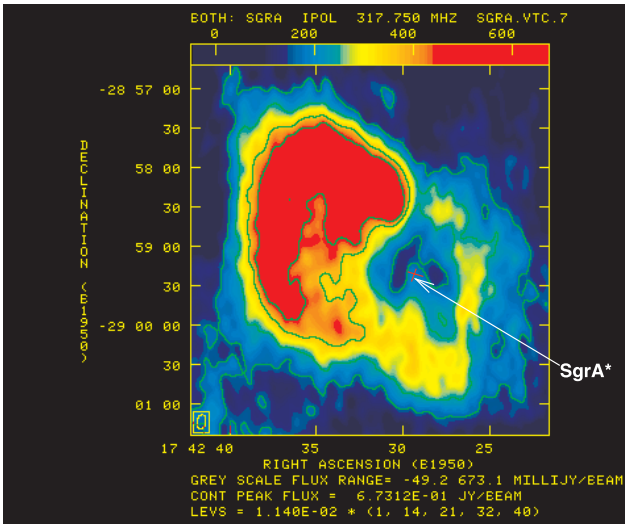

FIG. 1.—Pseudocolor/contour image of Sgr A* at 90 cm. *Contours*: 11.4 × 1, 14, 21, 32, and 40 mJy beam^{-1}. In order to compare our results with those obtained by Nord et al. (2004) at the same wavelength, we have restored the final image using a similar synthesized beam, i.e., 10.″9 × 6.″8 (P.A. = −10°). The rms noise in the image is 12 mJy beam^{-1}. The red cross at the image center marks the expected scattering size and position of Sgr A* at 90 cm, i.e., ~11″ × 6″ at P.A. = 80° (Rogers et al. 1994; Lo et al. 1998).

3.1. *Flux Density Measurement of Sgr A* at* 90 cm

Figure 1 shows the central 4.′5 region of the Galaxy at 90 cm. The supernova Sgr A East dominates the total flux density at 90 cm. An excess in flux density is observed at the expected location of Sgr A* (red cross at the image center in Fig. 1); the region surrounding Sgr A* is significantly absorbed by the ionized gas in Sgr A West, except for the extended emission south of Sgr A*. We made two slices along the major (P.A. = 80°) and minor (P.A. = −10°) axes of the expected scattering shape to determine the flux density of Sgr A* (Fig. 2). Gaussian profiles were fitted to each of the slices after subtracting diffuse emission from the background; an apparent size of (16.″0 ± 1.″3) × (15.″3 ± 2.″5) was determined. The errors in the parameters are determined using the two-dimensional Gaussian fitting procedure `jmfit` in AIPS and also checked by fitting the two one-dimensional slices (Fig. 2). The source size of Sgr A* at 90 cm is (14.″4 ± 1.″4) × (10.″7 ± 2.″4) and P.A. = 95° ± 25°, after deconvolution. The fitted peak flux density is 65 ± 16 mJy beam^{-1}, with a total flux density of 220 ± 60 mJy. The observed flux density and source size of Sgr A* at 90 cm agree with the determinations of Nord et al. (2004) within 1 σ.

3.2. *Simultaneous Spectrum on 2003 June 17*

Figure 3 shows the quasi-simultaneous spectrum of Sgr A* at wavelengths ranging from 90 cm to 3.8 μm, observed on 2003 June 17. Table 2 summarizes the flux density measurements. A rising spectrum extends from ~2 cm to the submillimeter band.

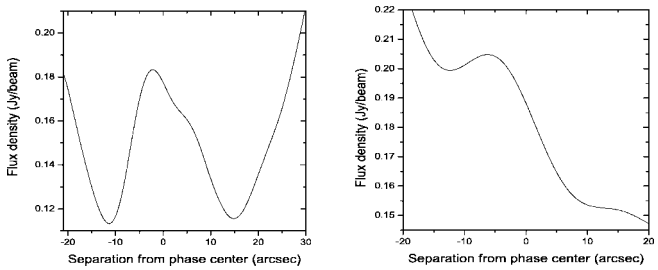

FIG. 2.—Crosscuts along the expected axes of Sgr A* at 90 cm. The slices are centered at R.A. = $17^h42^m29.^s4$, decl. = −28°59′18″ (B1950). *Left:* Slice through the major axis (P.A. = 80°) with a resolution of 6.″8. East is to the left. *Right:* Slice through the minor axis (P.A. = −10°) with a resolution of 10.″9. South is to the left.

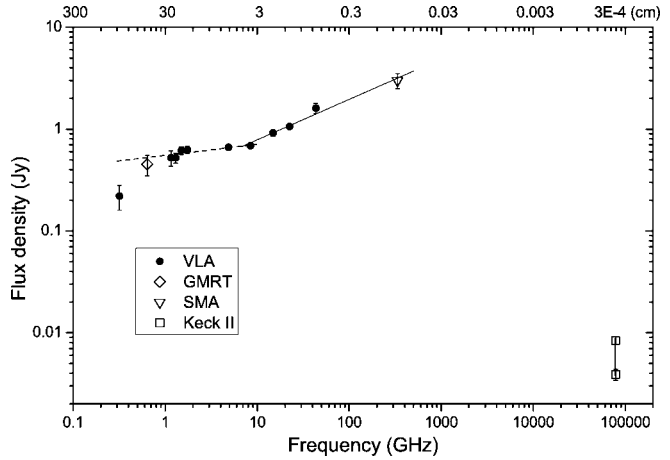

FIG. 3.—Simultaneous spectrum of Sgr A* from 90 cm to 3.8 μm on 2003 June 17. *Filled circle*, VLA; *diamond*, GMRT; *triangle*, SMA (J.-H. Zhao 2005, private communication); *square*, Keck II (Ghez et al. 2004).

However, the wavelength of the peak emission is quite uncertain since there are no measurements from 0.89 mm to 3.8 μm. The rising spectrum from the short cm to mm wavelengths can be described by a power law ($S_\nu \propto \nu^\alpha$) with $\alpha^{3.6\,\mathrm{cm}}_{0.89\,\mathrm{mm}} = 0.43 \pm 0.04$ (Fig. 3, *solid line*); the spectrum between 3.6 and 47 cm is flatter, $\alpha^{47\,\mathrm{cm}}_{3.6\,\mathrm{cm}} = 0.11 \pm 0.03$ (Fig. 3, *dashed line*). The difference in spectral indices between the two parts of the power-law spectra is $\alpha^{3.6\,\mathrm{cm}}_{0.89\,\mathrm{mm}} - \alpha^{47\,\mathrm{mm}}_{3.6\,\mathrm{mm}} = 0.32 \pm 0.05$, suggesting a significant break near 3.6 cm on 2003 June 17.

A break in the centimeter-band spectrum of Sgr A* has been suggested previously (Zylka et al. 1992; Falcke et al. 1998; Zhao et al. 2003). The determined break wavelength of 3–4 cm is consistent with the previously suggested break of 2–3.5 cm suggested by Falcke et al. (1998). The excess in flux density toward short wavelengths in the spectrum of Sgr A* might be associated with activities in the inner region of the accretion disk or jet nozzle (Melia & Falcke 2001). In comparison with the radio light curves, the increased spectral index at wavelengths shorter than the break of ~3.6 cm on 2003 June 17 is consistent with the fact that Sgr A* was undergoing a large radio outburst. The VLA monitoring campaign (Herrnstein et al. 2004) did show that Sgr A* was in an outburst stage at 7 mm near the epoch of 2003 June 16; the outburst apparently peaked near the epoch of 2003 July 17. The flux density at 7 mm on 2003 July 17 was at the highest level between 2000 June 21 and 2003 October 16 (Herrnstein et al. 2004). Therefore, a break in the spectrum of Sgr A* at a short centimeter wavelength could be a signature of synchrotron self-absorption (Kellermann & Pauliny-Toth 1969) of a relatively strong radio outburst, as proposed to explain the 2002 October 3 X-ray event and corresponding radio outburst (Zhao et al. 2004).

At 90 cm, the measured flux density of 0.22 ± 0.06 Jy is far below the inferred 0.49 Jy extrapolated from the power law fit $S_\nu \propto \nu^{0.11 \pm 0.03}$. This significant decrease (>4 σ) in flux density suggests that the spectrum of Sgr A* on 2003 June 17 could have a cutoff at wavelengths longer than 47 cm.

4. DISCUSSION

The earlier Jodrell Bank measurements of Sgr A* made by DWB showed a low-frequency turnover at about 1 GHz. The flux densities of 0.26 ± 0.03 Jy at 0.96 GHz and 0.56 ± 0.06 Jy at 1.66 GHz had been corrected for resolutions of the interferometer and the known angular diameters of Sgr A*. We note that the angular diameters measured with the Jodrell Bank at 0.96 and 1.66 GHz are consistent with the values extrapolated from the relationship between the angular size and observing wavelength (e.g., Lo et al. 1998; Bower et al. 2004). For angular sizes of 1.″5 at 0.96 GHz and 0.″5 at 1.66 GHz, Sgr A* is dominant on baselines from 34 to 75 kλ and from 60 to 132 kλ, respectively. The errors in flux densities at these two frequencies (~10%) are consistent with those estimated from our current data at 20 cm. However, the 408 MHz upper limit measured by DWB with a single baseline is quite uncertain because of confusion arising from the complex region in Sgr A East in close proximity to the broadened source Sgr A* at 408 MHz (e.g., ~8′, Roy & Rao 2004). This upper limit will be excluded in following discussion.

TABLE 2

FLUX DENSITY DETERMINATIONS OF SGR A* ON 2003 JUNE 17

λ (cm)	S (Jy)	σ_T (Jy)	σ_C (%)	σ_M (%)
90	0.22	0.06	10	25
47	0.45	0.10	10	20
26	0.52	0.09	3	17
23	0.52	0.06	4	11
20	0.62	0.06	5	7
17	0.63	0.05	5	6
6	0.66	0.04	4	4
3.6	0.69	0.03	4	2
2	0.92	0.06	7	1
1.3	1.06	0.06	5	2
0.7	1.6	0.2	11	1

Figure 4 shows the observed spectra for Sgr A* at epochs 1975 (DWB) and 2003 (this Letter) for wavelengths longer than 3.6 cm. A ratio of 2.0 ± 0.4 [$S_{1.16\,\mathrm{GHz}}(2003)/S_{0.96\,\mathrm{GHz}}(1975)$] would suggest a significant increase in the flux density at about 1 GHz from epoch 1975 to 2003. The spectra at both epochs can be fitted with a model of a slowly rising power-law spectrum ($\propto\nu^\alpha$) together with a free-free absorption screen ($e^{-\tau_{\mathrm{ff}}}$) between Sgr A* and the observer, as first proposed by DWB. If the flux density at 0.96 GHz measured by DWB is indeed reliable, then the comparison of the fits to the 1975 (Fig. 4, *dashed line*) and 2003 data (Fig. 4, *solid line*) does suggest a substantial change in the spectrum of Sgr A* at wavelengths longer than 30 cm in the past 28 years.

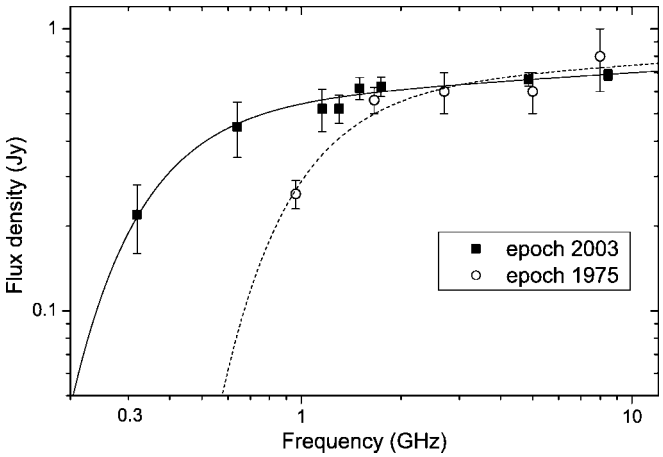

FIG. 4.—Comparison of the low-frequency spectra of Sgr A* observed between epochs 2003 (*filled square*) and 1975 (*open circle*). The dashed and solid lines represent fits using free-free absorption opacity to the spectrum at epochs 1975 and 2003, respectively. The free-free opacity decreases by a factor of ~9 at 30 cm from 1975 to 2003.

If the free-free absorption model is in fact correct, the variation in the low-frequency spectrum would suggest that the column density of the free-free absorption screen must have decreased significantly over the past 28 years. Starting from DWB's free-free absorption model ($S_\nu \propto \nu^\alpha e^{-\tau_{\rm ff}}$), the quantitative change in the column density of ionized gas in front of Sgr A* can be assessed. The data observed at both epochs can be fitted with a power-law spectrum $S_\nu \propto \nu^{0.074\pm0.022}$ at the higher frequencies along with an exponential cutoff at the lower frequencies arising from free-free absorption. The comparison of the model fits to the observations at these two epochs suggests that free-free absorption opacity ($\tau_{\rm ff}$) toward Sgr A* must have decreased by a factor of 9 from 1975 to 2003. The critical cutoff in wavelength due to free-free absorption has changed from ~30 to ~100 cm. Assuming the electron temperature of the ionized gas remains constant, the inferred decrease in $\tau_{\rm ff}$ would then correspond to a decrease by a factor of 9 in emission measure EM $= \int n_e^2\, dl$. Such a large variation in EM is unlikely to arise from changes in electron density in the halo of Sgr A East (Pedlar et al. 1989).

If the changes in EM and electron density do occur in a compact region within 0.″1–10″ of Sgr A* (0.004–0.4 pc), stellar winds which originate from massive stars toward Sgr A* could provide the changing environment. For example, Loeb (2004) suggested that stellar winds from the close-in stars could modulate low-frequency flux density of Sgr A* over a timescale of about ten years through orbital motions of the stars. Here we consider two types of stellar winds: (1) the stellar wind is isotropic ($n_e \propto r^{-2}$) and (2) the stellar wind forms a one-dimensional flow due to the gravity of the SMBH ($n_e \propto r^{-1}$). Using the star S2 (Schödel et al. 2002) as an example, the orbit period is about 15 years and the ratio of the pericenter and apocenter is about 1:15; the star has a surface temperature of about 30,000 K, providing an ionization zone of H roughly equivalent of a B0 star (Ghez et al. 2003). The stellar wind mass flux at pericenter in case (1) is about 200 times that at apocenter; in case (2) the ratio in stellar wind flux between pericenter and apocenter is 15:1. The ratio of 3:1 in electron column density between 1975 and 2003 inferred from the change of the low-frequency cutoff is much less than that of the stellar wind flux in both cases. Nevertheless, large amplitude fluctuations of accreted matter within 0.002 pc (0.″05) captured from the stellar winds near Sgr A* over a timescale of less than a few decades were predicted in numerical simulations (Melia & Coker 1999). A variation in the radio continuum spectrum was also suggested by the simulations, although the authors attributed the low-frequency turnover to refraction effects. It is more likely that the source for the low-frequency turnover is free-free absorption from cool gas in close proximity to Sgr A*. The colder gas (~10^4 K) can coexist with the hot gas (~10^7 K) that provides the X-ray emission near Sgr A* (Cuadra et al. 2005a, 2005b). For a stellar wind with a size of 0.004 pc, the free-free absorption opacity is about unity at about 0.4 GHz for an electron density of 10^4 cm^{-3} and electron temperature of 10^4 K. The variation of the low-frequency turnover due to free-free absorption toward Sgr A* appears to be sensitive to fluctuations of the stellar wind mass captured by the SMBH potential.

We thank the referee and H. Falcke for helpful comments. The work is supported by the NSFC (10503008, 10328306, 10333020). The VLA is operated by the National Radio Astronomy Observatory, a facility of the National Science Foundation operated under cooperative agreement by Associated Universities, Inc. The GMRT is a component of the National Centre for Radio Astrophysics of the Tata Institute of Fundamental Research.

REFERENCES

Baars, J. W. M., Genzel, R., Pauliny-Toth, I. I. K., & Witzel, A. 1977, A&A, 61, 99
Balick, B., & Brown, R. L. 1974, ApJ, 194, 265
Bower, G. C., Falcke, H., Herrnstein, R. M., Zhao, J.-H., Goss, W. M., & Backer, D. C. 2004, Science, 304, 704
Coker, R. F., & Melia, F. 1997, ApJ, 488, L149
Cuadra, J., Nayakshin, S., Springel, V., & Di Matteo, T. 2005a, MNRAS, 360, L55
———. 2005b, MNRAS, submitted (astro-ph/0505382)
Davies, R. D., Walsh, D., & Booth, R. S. 1976, MNRAS, 177, 319 (DWB)
Falcke, H., Goss, W. M., Matsuo, H., Teuben, P., Zhao, J.-H., & Zylka, R. 1998, ApJ, 499, 731
Ghez, A. M., et al. 2003, ApJ, 586, L127
———. 2004, ApJ, 601, L159
Herrnstein, R. M., Zhao, J.-H., Bower, G. C., & Goss, W. M. 2004, AJ, 127, 3399
Ho, P. T. P., Moran, J. M., & Lo, K. Y. 2004, ApJ, 616, L1
Kellermann, K. I., & Pauliny-Toth, I. I. K. 1969, ApJ, 155, L71
Lo, K. Y., Shen, Z.-Q., Zhao, J.-H., & Ho, P. T. P. 1998, ApJ, 508, L61
Loeb, A. 2004, MNRAS, 350, 725
Melia, F., & Coker, R. F. 1999, ApJ, 511, 750
Melia, F., & Falcke, H. 2001, ARA&A, 39, 309
Moran, J. M. 1998, Proc. SPIE, 3357, 208
Nord, M. E., Lazio, T. J. W., Kassim, N. E., Goss, W. M., & Duric, N. 2004, ApJ, 601, L51
Pedlar, A., et al. 1989, ApJ, 342, 769
Rogers, A. E. E., et al. 1994, ApJ, 434, L59
Roy, S., & Rao, A. P. 2004, MNRAS, 349, L25
Schödel, R., et al. 2002, Nature, 419, 694
Zhao, J.-H., Herrnstein, R. M., Bower, G. C., Goss, W. M., & Liu, S. M. 2004, ApJ, 603, L85
Zhao, J.-H., et al. 2003, ApJ, 586, L29
Zylka, R., Mezger, P. G., & Lesch, H. 1992, A&A, 261, 119